

Identification of optimum conditions for zinc electrowinning in high-purity synthetic electrolytes

E. J. FRAZER

CSIRO Institute of Energy and Earth Resources, Division of Mineral Chemistry, PO Box 124, Port Melbourne, Victoria 3207, Australia

T. LWIN

CSIRO Institute of Physical Sciences, Division of Mathematics and Statistics, Private Bag 10, Clayton, Victoria 3168, Australia

Received 10 April 1986

The optimum conditions for zinc electrowinning in synthetic acidic zinc sulphate electrolytes (0.8 M ZnSO₄ + 1.07 M H₂SO₄) were determined using response surface statistical analysis. The coulombic efficiency (QE) was optimized with respect to temperature (T), current density (J) and electrode rotation rate (n). For an electrolyte prepared from AR zinc sulphate and Aristar sulphuric acid, containing trace lead and nickel, QE reached a maximum of 98.8% on a zinc substrate under the following conditions: $T = 50^\circ\text{C}$, $J = 500\text{ A m}^{-2}$, $n = 35\text{ s}^{-1}$. For a very-high-purity electrolyte, prepared by dissolution of 99.9999% zinc in Aristar sulphuric acid, a maximum QE of 98.4% was predicted and obtained at: $T \simeq 61^\circ\text{C}$, $J \simeq 890\text{ A m}^{-2}$, $n \simeq 38\text{ s}^{-1}$. Using a statistical response surface model calculated during the optimization process, QE contours giving an overall view of electrolyte performance were constructed. The QE responses were determined principally by T and J , with significant interaction between n and J or T and J , depending on the impurity composition of the electrolyte. The model was also used to predict the QE response of the above electrolytes under conditions similar to industrial practice.

1. Introduction

Laboratory studies on zinc electrowinning are in general concerned with the influence of certain impurities on coulombic efficiency (QE) and zinc deposit morphology. Studies dealing with the effect of electrodeposition conditions alone for an electrolyte of fixed impurity composition are less frequent and have usually been conducted on a 'one factor at a time' basis [1-5]. The trends observed may be quite useful since, in the industrial situation, there is often only a small range over which electrodeposition conditions can be varied. Unfortunately, such investigations provide little information about possible interactions between electrodeposition variables and do not allow the assessment of electrolyte performance over a wide range of conditions. However, at least three studies [6-8] have used

multivariate statistical techniques to characterize electrolyte performance. Kulikov [6] generated QE contours as a function of current density and sulphuric acid concentration for an industrial zinc electrolyte. Villas Bôas [7] used factorially designed experiments to investigate the effect of pH, zinc concentration, current density and trace silver on zinc electrodeposition; various first- and second-order interactions between these factors were shown to be influencing both QE and cathode potential. Fosnacht and O'Keefe [8] used a two-level factorial design to study the effect of several impurities, glue, temperature and acidity in both commercial and synthetic zinc electrolytes. The latter study revealed interactions not only between the electrolyte impurities themselves (e.g. cobalt and arsenic), but also between the impurities, temperature and acidity.

In a previous communication [9] the QE for zinc electrodeposition was investigated with regard to intrinsic electrolyte purity, as judged by anodic stripping voltammetry (ASV) and the inductively coupled plasma (ICP) technique. While much of that work was carried out under a fixed set of electrolysis conditions, it was also necessary to establish the conditions under which QE approached a maximum and whether these depend on electrolyte purity. Maximization was carried out as a function of temperature (T), current density (J) and electrode rotation rate (n revolutions per second) for two electrolytes of different impurity compositions. In this communication we give details of that maximization process and the statistical methods employed [10–12]. In addition to defining the upper limit for QE, the data were also used to generate QE contours over a wide range of electrodeposition conditions and to characterize and predict the performance of two electrolytes under conditions closer to plant practice.

2. Experimental details

The glass electrochemical cell and the fabrication and preparation of the aluminium and zinc rotating disc electrodes ($\sim 2\text{ cm}^2$) have been described previously [9, 13]. The zinc electrolytes were prepared from BDH Aristar H_2SO_4 and either Merck AR $\text{ZnSO}_4 \cdot 7\text{H}_2\text{O}$ or Koch–Light 99.9999% zinc. The electrolyte prepared using the AR zinc sulphate (the ‘baseline’ electrolyte) contained ~ 1.2 p.p.m. lead and 0.2 p.p.m. nickel as major impurities, while the electrolyte prepared from the 99.9999% Zn (the ‘very-high-purity’ electrolyte) contained almost no detectable impurities, as evaluated by ASV and ICP [9]. In the latter case the zinc metal was dissolved in sulphuric acid solution while in contact with a platinum grid. The electrolyte composition was fixed at $0.8\text{ M ZnSO}_4 + 1.07\text{ M H}_2\text{SO}_4$ and the solution was deoxygenated before zinc electrodeposition.

The QE for zinc electrodeposition was determined as before [9, 13] from the weight of zinc deposited under mass-transfer-controlled conditions (Tacussel Type EDI electrode rotator) after the passage of $\sim 600\text{ C}$ ($\sim 200\text{ mg}$ zinc). Although there was only minor depletion of the

zinc concentration at the end of a deposition run ($\sim 3\%$), fresh solution was used for each QE determination. An aluminium substrate was normally employed, but a zinc substrate was substituted when optimum conditions were identified, to eliminate the small effect a foreign substrate has on QE [9]. A PAR 173 potentiostat/galvanostat equipped with a PAR 179 digital coulometer was employed as the constant-current source.

3. Results and discussion

3.1. Identification of optimum conditions

The general approach to the optimization of QE adopted here is based on that of Box and Wilson [10], as summarized in a later compilation [11]. The experimental limits for the process variables (factors) are decided and an initial small experiment is carried out in a reasonable sub-region chosen by experience. This is based on either a whole or half replicate of a factorial design with two levels in each of the factors. Based on the data of this (first) experiment (E1), a ‘path of steepest ascent’ towards a plausible optimum is determined. Along this path, a few points are chosen to determine the likely centre of a second experiment (E2). Depending on the results obtained at this stage, the levels and/or the ranges of the factors in E2 are changed to cover a new sub-region. If the data of E2 exhibit a reasonable proximity to a local optimum, extra design points are chosen to complement the basic factorial design to obtain enough data to fit a quadratic surface. If necessary, a new path of steepest ascent is calculated from the data of E2 and the procedure is repeated to obtain a centre for a third experiment (E3), and so on.

With sufficient data, a quadratic model may be fitted at any stage of the sequential experiment and a test of optima (maxima) applied. If the test indicates a maximum, one can stop the sequence and obtain a final fitted model of all combined data. If the quadratic surface fails to produce a maximum, one can still obtain a constrained optimum over a prescribed region [14]. This later modification to the optimization process is especially useful if, at any stage, further data collection is impossible due to

Table 1. Design points and corresponding coulombic efficiencies for baseline electrolyte

Experiment	T (°C)	n (s ⁻¹)	J (A m ⁻²)	QE (%)
E1	25	10	300	97.5
	25	10	400	97.5
	25	20	300	97.5
	25	20	400	97.6
	35	10	300	98.0
	35	10	400	97.9
	35	20	300	98.1
	35	20	400	98.0
Path	40	18	330	98.1
	45	20	320	98.3, 98.3
	50	22	310	98.3
	55	24	300	98.0
E2	40	5	140	98.1
	40	5	500	97.9
	40	35	140	97.4
	40	35	500	98.4
	50	5	140	98.0
	50	5	500	98.1
	50	35	140	97.2
	50	35	500	98.5
	45	46	320	98.3
	45	20	630	98.3
	36	20	320	98.4, 98.3
	54	20	320	98.4
	Supplementary design points	51	38	320
39		38	320	98.4
35		55	400	98.4
40		20	400	98.2
45		20	400	98.1

experimental or other constraints [15]. Also, it is quite possible that a locally fitted quadratic surface may produce a maximum whereas that fitted on a combined data set, covering a wide experimental region, may not. In this case the constrained optimization technique may still be applied.

3.2. Maximization of QE in the baseline electrolyte

At an earlier stage, as a test of repeatability of the apparatus and methodology, 12 repeat runs were carried out to determine QE under identical 'standard conditions', namely $T = 25^\circ\text{C}$, $n = 20\text{ s}^{-1}$ and $J = 400\text{ A m}^{-2}$. The error variance

(σ^2) of these QE values was 0.015 giving a standard deviation (σ) of 0.12%. This error variance was taken as a bench mark value for the true total measurement error of QE after independent checks on its likely value by a propagation of error technique. In the following analyses, when statistical significance tests were performed, we use the above value of σ as the standard deviation of the residual error of the fitted response surface.

The first experiment (E1) performed was a 2^3 factorial design whose levels are given in Table 1 (E1). An analysis of variance technique was carried out on the data of E1 and T was found to be the only statistically significant factor. A path of steepest ascent was calculated through the least squares fitted model given below:

$$\text{QE} = b_0 + b_1t + b_2N + b_3j + b_4(tN) + b_5(tj) + b_6(Nj) + \text{error} \quad (1)$$

where $t = (T - 30)/5$, $N = (n - 15)/5$, $j = (J - 350)/50$ and the regression coefficients $b_0, b_1 \dots b_6$ are given in Table 2, column 3. Determinations of QE were made at four selected points (see Table 1) on the path and, based on these observations, a decision was made to choose the centre of E2 at $T = 45^\circ\text{C}$, $n = 20\text{ s}^{-1}$ and $J = 320\text{ A m}^{-2}$.

The second experiment (E2) performed was a complete 2^3 factorial design which was later complemented by four of the star design points (see [12] for the star design); the levels of this experiment are given in Table 1 (see E2). With the magnitude of units for n and J increased, it was now seen that none of the effects of T , J and n could be ignored. The effect of interactions between T and J and between n and J became statistically significant. The data of E2 and the four points along the path of ascent were combined to obtain a least squares fitted model as follows:

$$\text{QE} = b_0 + b_1t + b_2N + b_3j + b_4(tN) + b_5(tj) + b_6(Nj) + b_7t^2 + b_8N^2 + b_9j^2 + \text{error} \quad (2)$$

where $t = (T - 45)/5$, $N = (n - 20)/15$ and $j = (J - 320)/180$ and the regression coefficients $b_0, b_1 \dots b_9$ are given in Table 2, column 4.

Table 2. Baseline electrolyte: regression coefficients of various statistical models

Scaled variable	Coefficient	E1	E2	All data combined ^a	
Constant	b_0	96.81	98.3	98.27	-
t	b_1	0.3125	0.0000	0.0069	(0.31)
N	b_2	0.0375	-0.0352	-0.0193	(-0.44)
j	b_3	-0.0375	0.3148	0.2883	(6.23)
tN	b_4	0.0375	-0.025	-0.0324	(-1.17)
tj	b_5	0.1125	0.0750	0.0730	(1.90)
Nj	b_6	-0.0125	0.3000	0.2910	(5.82)
t^2	b_7	-	0.0027	-0.0401	(-4.67)
N^2	b_8	-	-0.0409	-0.0207	(-0.61)
j^2	b_9	-	-0.2430	-0.2125	(-4.49)

^a Values of the Student's t statistic are indicated in brackets; the table value for comparison is 2.07 at the 95% level of confidence for 22 degrees of freedom.

While the second order coefficients have generally become statistically significant, as expected, the resulting stationary point of the response surface was not a maximum. This is due to the fact that a high value of QE (98.5%) was observed at a 'corner' ($T = 50^\circ\text{C}$, $n = 35\text{ s}^{-1}$, $J = 500\text{ A m}^{-2}$) of E2.

To obtain a more representative response surface for the experimental region under consideration, it was decided to combine the data of E1 and E2 plus observations on the path. Further data points were obtained to supplement this combination and are shown in Table 1. The quadratic model of the form given in Equation 2 was then fitted to the combined data; the resulting regression coefficients are given in Table 2, column 5. The data added to those of E2 generally give more information on lower temperatures and, therefore, the fitted response surface did not produce a stationary point which

was also a maximum. The highest observed QE values were still at a 'corner' of the experimental region covered by the combined data.

Analysis of the combined data also indicated that the effect of T was the most pronounced followed by that of J , and that the effect of n was significant only through its interaction with J . Further, it was experimentally verified that for a given T , a low n requires a high J to sustain the same QE. Among the interactions, that between n and J is most pronounced, followed by that between T and J . QE contours for combinations of n and J at $T = 35$ or 55°C are given in Fig. 1.

Further experimentation to determine conclusively the optimum deposition conditions was not carried out due to lack of the same batch of AR zinc sulphate. The best possible QE (98.5%) obtained at $T = 50^\circ\text{C}$, $n = 35\text{ s}^{-1}$ and $J = 500\text{ A cm}^{-2}$ in the experiment was, however, regarded as being near-optimum due to the

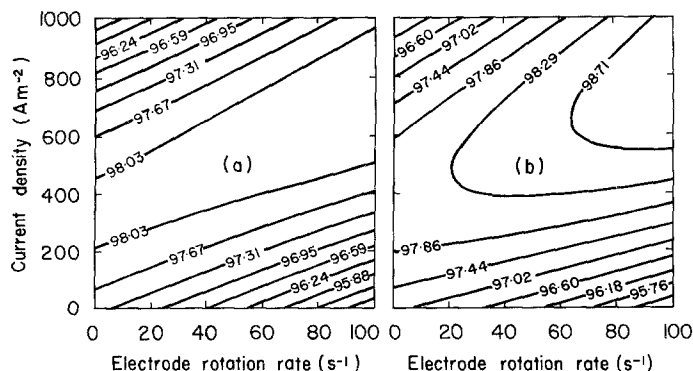


Fig. 1. QE response surface as a function of J and n . Electrolyte, AR $\text{ZnSO}_4 \cdot 7\text{H}_2\text{O}/\text{BDH}$ Aristar H_2SO_4 ; 2 cm^2 aluminium cathode. (a) $T = 35^\circ\text{C}$; (b) $T = 55^\circ\text{C}$.

Table 3. Design points and corresponding coulombic efficiencies for very-high-purity electrolyte

Experiment	T (°C)	n (s ⁻¹)	J (A m ⁻²)	QE (%)
E1	30	20	500	97.5
	30	40	300	97.6
	40	20	300	97.7
	40	40	500	98.0
	35	30	400	97.7
Path 1	40	37.4	436	97.8
	50	52.1	508	98.0
	60	66.8	579	97.6
E2	39	54.7	372	97.7
	51	54.7	572	97.9
	39	34.7	572	97.7
	51	34.7	372	97.7
	45	44.7	472	97.8
Path 2	55	60.1	638	98.0
	57.5	63.9	680	98.0
E3	32.5	30.5	485	97.7
	32.5	59.5	485	97.6
	32.5	30.5	715	97.5
	32.5	59.5	715	97.5
	52.5	30.5	485	98.0
	52.5	59.5	485	97.9
	52.5	30.5	715	98.2
	52.5	59.5	715	98.1
	42.5	45.0	600	97.8, 97.8
	60.0	45.0	600	98.2
	42.5	45.0	800	97.8
	42.5	70.0	600	97.8
	42.5	45.0	400	97.8
	42.5	20.0	600	97.7
	25.0	45.0	600	96.8
	25.0	20.0	400	97.0, 97.1, 97.1
	60.0	70.0	800	97.9
	Path 3 + supplementary points	55.0	27.2	600
55.0		45.0	741	98.2
42.5		27.2	741	97.5
62.5		41.1	616	98.0
E4	52.5	30.5	815	98.1
	57.5	45.0	765	98.3
	62.5	30.5	715	98.2
	62.5	59.5	815	98.1

remarkable flatness of the response surface at high T ; a further increase in QE to 98.8% was observed under the same conditions when using a zinc substrate.

3.3. Maximization of QE in the very-high-purity electrolyte

It should be noted that for the very-high-purity electrolyte, sequential experiments were necessarily conducted with solutions prepared from different zinc rods which are bound to have slightly varying impurity compositions (although nominally of the same batch) and hence there is 'batch-to-batch' variation in QE [9]. In this case, repeat runs under standard conditions (25°C, 20 s⁻¹, 400 A m⁻²) were monitored to give a check on the repeatability of the QE determination.

Although analysis of data in E3 and all combined data (see Table 3) involved several different zinc rods, the residual variance (0.021) after fitting a required quadratic surface was only slightly larger than the replicate error variance determined in Section 3.2. Thus, this residual variance was used as a new error variance in these analyses instead of performing a more complicated analysis requiring different variances for runs with different batches.

The first experiment (E1) performed was a half replicate plus the centre point of a 2³ factorial design. The levels of the factors used are given in Table 3 (E1). The model (Equation 1) was fitted without the interaction terms since only five data points were available. It should be used with $t = (T - 35)/5$, $N = (n - 30)/10$ and $j = (J - 400)/100$, together with the regression coefficients given in Table 4, column 3. The effect of T was seen to be the most pronounced and was the only statistically significant factor. A path of steepest ascent based on the data of E1 was calculated and three points (Table 3, path 1) were chosen corresponding to $T = 40, 50$ and 60°C . Based on QE determinations at these points, the centre of the next experiment was chosen at $T = 45^\circ\text{C}$, $n = 44.7\text{ s}^{-1}$ and $J = 472\text{ A m}^{-2}$.

The second experiment (E2) performed was also a half replicate plus the centre point of a 2³ factorial design. It was performed such that the first-order effects could be estimated as soon as QE determinations were made at a relevant set of design points. A model of the form given in Equation 1 was fitted with $t = (T - 45)/6$, $N = (n - 44.7)/10$, $j = (J - 472)/100$ and the

Table 4. Very-high-purity electrolyte: regression coefficients for various models

Scaled variable	Coefficient	E1	E2	E3	All data combined ^a	
Constant	b_0	97.67	97.74	97.85	97.89	—
t	b_1	0.1325	0.0625	0.3063	0.2680	(10.05)
N	b_2	0.0475	0.0625	-0.0288	-0.0281	(-1.05)
j	b_3	0.0975	0.0575	-0.0073	-0.0161	(-0.65)
tN	b_4	—	—	-0.0478	-0.0386	(-1.39)
tj	b_5	—	—	0.0569	0.1185	(4.20)
Nj	b_6	—	—	-0.0052	0.0211	(0.80)
t^2	b_7	—	—	-0.1018	-0.1150	(-4.65)
N^2	b_8	—	—	-0.0097	-0.0421	(-1.49)
j^2	b_9	—	—	-0.0002	-0.0369	(-1.92)

^a Values of the Student's t statistic are indicated in brackets; the table value for comparison is 2.02 at the 95% level of confidence for 39 degrees of freedom.

coefficients representing the first-order effects are given in Table 4, column 4. Following calculation of a path of steepest ascent, two determinations of QE were made along the path (see Table 3, path 2). Based on the data obtained, it was decided to move the centre of the next experiment to $T = 42.5^\circ\text{C}$, $J = 600\text{ A m}^{-2}$ and $n = 45\text{ s}^{-1}$. The decision to move to a slightly lower temperature was made for two reasons. The data on the path did not exhibit a significant rise in QE even at 57.5°C and it was necessary to locate a centre such that when the appropriate units for T were considered, the upper extremity of the design did not exceed the experimentally feasible upper limit of T . Also, some instrumental problems were encountered at an early stage of the experiment at high temperatures which suggested caution in approaching high values of T .

The next experiment (E3) was a complete 2^3 factorial design supplemented by the following design points: (i) the centre point (two replicates); (ii) the six design points corresponding to a star design of Box *et al.* [12]; and (iii) two extra design points (two replicates each) carried out to gauge the extent of experimental problems of operating at high T . The design points are given in Table 3 (see E3). A quadratic model of the form given in Equation 2 with $t = (T - 42.5)/10$, $N = (n - 45)/14.5$ and $j = (J - 600)/115$ was fitted to the data of 20 design points and the resulting regression coefficients are given in Table 4, column 5. For n and J , the second-order effects are much more pronounced than the first-

order effects. But for T , the first-order effect is still more pronounced than the second-order effect, indicating a possibility of further improvement in QE at even higher temperatures. This was confirmed by a separate analysis based on all data points from the paths and E3 with $T \geq 39^\circ\text{C}$. These results indicated that virtually all second-order effects were statistically significant and that, except for T , all first-order effects were not statistically significant; hence a movement of the centre to higher temperatures was indicated.

Although the centre for the final experiment (E4) should have had $T \approx 60^\circ\text{C}$ (as indicated by a further calculated path of steepest ascent based on data of E3), experimental problems at high temperatures (e.g. electrode leakage) did not allow this. Thus, it was decided to have a centre at $T = 57.5^\circ\text{C}$, $J = 765\text{ A m}^{-2}$ and $n = 45\text{ s}^{-1}$. The levels of the factors were decided in such a way that one corner point of the 2^3 factorial design embedded in E3 also became a corner point of the following 2^3 design (E4). This was done to reduce the total number of runs required in case the calculated path of ascent indicated a further move.

Only a half replicate of the 2^3 design was carried out as E4, with levels as indicated in Table 3. A path of steepest ascent was calculated and the results suggested no further improvement by changing the centre of the experiment. A quadratic model of the form given in Equation 2 was fitted to all available data with $T \geq 50^\circ\text{C}$.

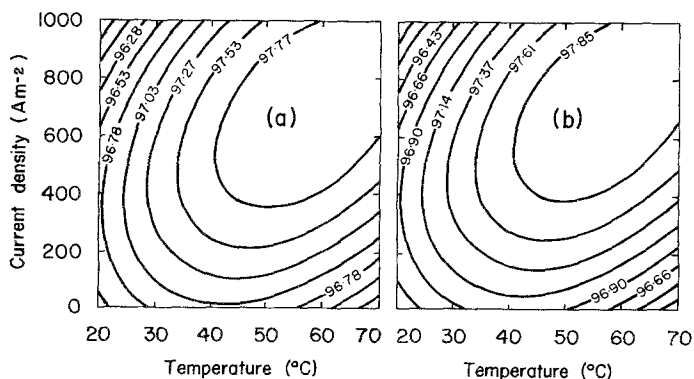


Fig. 2. QE response surface as a function of T and J . Electrolyte, 99.9999% zinc/BDH Aristar H_2SO_4 ; 2 cm^2 aluminium cathode. (a) $n = 20\text{ s}^{-1}$; (b) $n = 40\text{ s}^{-1}$.

The resulting fitted response surface exhibits a stationary point which is also a maximum. This design point was given by $T = 60.8^\circ\text{C}$, $n = 38.37\text{ s}^{-1}$ and $J = 890.9\text{ A m}^{-2}$, with a predicted QE value of 98.34% as against the actually observed value of 98.4%; in this case no further increase in QE was observed when a zinc substrate was substituted for aluminium.

Part of the objective of the sequential experiments was to explore the response surface to obtain a reasonably representative picture of QE with respect to variations in electrodeposition conditions. To this end a quadratic model of the form given in Equation 2 with $t = (T - 42.5)/10$, $N = (n - 45)/14.5$ and $j = (J - 600)/115$ was fitted to all available data. The regression coefficients for the fitted model are given in Table 4, column 6. Analysis of the combined data also indicated that the effect of T is most pronounced, followed by that of J , and that the interaction of T with J is most pronounced among the interactive effects. Typical QE contours for combinations of T and J at $n = 20$ or 40 s^{-1} are given in Fig. 2.

Although the quadratic surface fitted to all combined data did not produce a local unconstrained maximum, a constrained maximum of 98.4% was identified using the flexible simplex algorithm of Nelder and Mead [14] at $T = 65^\circ\text{C}$, $n = 37\text{ s}^{-1}$ and $J = 980\text{ A m}^{-2}$, for the region $25^\circ\text{C} \leq T \leq 65^\circ\text{C}$, $20\text{ s}^{-1} \leq n \leq 90\text{ s}^{-1}$, $200\text{ A m}^{-2} \leq J \leq 1000\text{ A m}^{-2}$. This indicates that, for the practical experimental region, the upper limit for QE is the same as the one achieved for the stationary design point identified above.

3.4. Prediction of electrolyte performance under plant conditions

Recently there have been attempts to model electrowinning cells [16, 17] and predict performance from first principles. Scott *et al.* [17] have significantly extended Bryson's model [16] to simulate the performance of a zinc electrowinning cell, using up to 200 variables; QE, energy consumption and dynamic response to a step change in process conditions can be calculated. The response surface model available here allows QE to be calculated as a function of T , J and n , with either one or two variables held constant, while still taking into account any interactive effects.

To allow predictions of electrolyte performance under conditions closer to plant practice, T and J were set to 35°C and 400 A m^{-2} , respectively. The QE was then calculated as a function of n and the predicted data are presented in Fig. 3 for both the baseline and very-high-purity electrolytes. The baseline electrolyte exhibits a monotonic increase in QE up to $n \approx 80\text{ s}^{-1}$; since trace lead apparently has a beneficial influence on QE [18, 19], this behaviour is probably due to the increasing lead concentration in the electrodeposited zinc as n is increased. The very-high-purity electrolyte exhibits a maximum in QE at $n \approx 40\text{ s}^{-1}$; this value represents a much higher mass transfer rate than that expected in practice. It is difficult to say whether the depicted trend in this case represents an intrinsic dependence of QE on n , or is perhaps due to interaction between residual beneficial and deleterious impurities. It is known that the hydrogen evol-

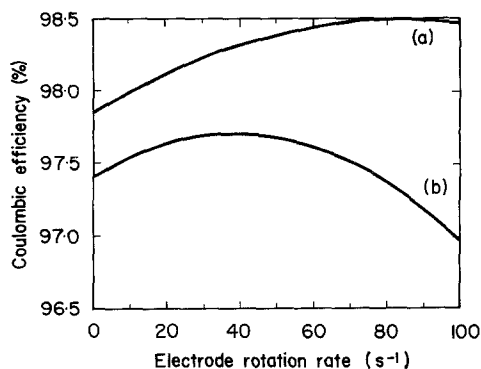


Fig. 3. QE as a function of n when $T = 35^\circ\text{C}$, $J = 400\text{ A m}^{-2}$ with a 2 cm^2 aluminium cathode. Electrolyte, BDH Aristar H_2SO_4 and (a) AR $\text{ZnSO}_4 \cdot 7\text{H}_2\text{O}$, (b) 99.9999% zinc.

ution reaction itself can be a function of mass transfer rate in acidic media (on platinum electrodes, at least [20]), and that effects due to residual impurities may still be present even in very-high-purity electrolytes [9]. In any case, the occurrence of the maximum allows the convenient choice of a region where the QE is relatively insensitive to changes in n for the examination of relationships between other factors.

Fig. 4 shows the predicted variations of QE with J for both electrolytes, with T and n held constant at 35°C and 40 s^{-1} , respectively. Both electrolytes exhibit a maximum in QE, but the maximum occurs at different values of J , namely $400\text{--}450$ and 550 A m^{-2} , for the very-high-purity and baseline electrolyte, respectively. The data in Fig. 4 for the very-high-purity electrolyte show that QE varies by only $\sim 0.2\%$ over the

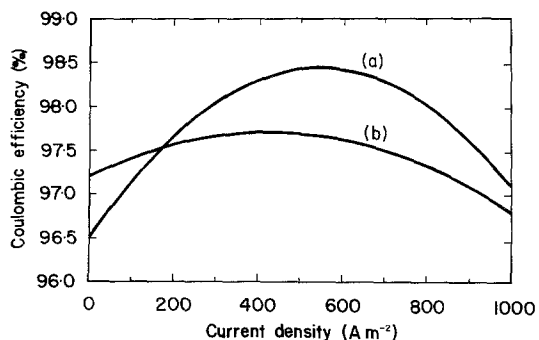


Fig. 4. QE as a function of J when $T = 35^\circ\text{C}$, $n = 40\text{ s}^{-1}$ with a 2 cm^2 aluminium cathode. Electrolyte, BDH Aristar H_2SO_4 and (a) AR $\text{ZnSO}_4 \cdot 7\text{H}_2\text{O}$, (b) 99.9999% zinc.

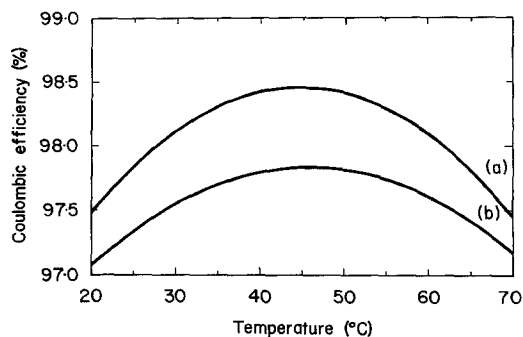


Fig. 5. QE as a function of T when $J = 400\text{ A m}^{-2}$, $n = 40\text{ s}^{-1}$ with a 2 cm^2 aluminium cathode. Electrolyte, BDH Aristar H_2SO_4 and (a) AR $\text{ZnSO}_4 \cdot 7\text{H}_2\text{O}$, (b) 99.9999% zinc.

range $300\text{--}700\text{ A m}^{-2}$. This confirms the independence of QE with J predicted by Scott *et al.* [17], for an electrolyte containing no impurities over the same range of J .

While there have been several experimental studies of the relationship between QE and J over a range of deposition conditions, the results in general have been inconsistent. Bratt [21] predicted an increase in QE with J , based on a derivation of 'Wark's Rule' [22]. Wark [22] observed an increase in QE from 87.0% at $J \approx 10\text{ A m}^{-2}$ to 97.4–97.6% at $300\text{--}900\text{ A m}^{-2}$ in a high-purity electrolyte, the latter result being in agreement with the present predictions. Turomshina and Stender [1] reported a similar increase in QE with J , with a maximum at $J \geq 1000\text{ A m}^{-2}$, while Liebscher [4] reported a maximum at $J \approx 450\text{ A m}^{-2}$. Salin [23] reported a small ($\sim 2\%$) but steady increase in QE with J over the range $100\text{--}1500\text{ A m}^{-2}$ at 20°C . Kulikov [6] analysed plant data (presumably) and reported a similar trend up to $\sim 1000\text{ A m}^{-2}$ for electrolytes of various acidities. Znamenskii and Stender [2] showed that the shape of the QE versus J curve was dependent on solution purity, with a plateau occurring at very low values of J ($\leq 100\text{ A m}^{-2}$) in pure solutions.

Taken together, the above predictions and experimental results strongly indicate that the potential beneficial influence on QE of any change in J from normal operating conditions ($400\text{--}600\text{ A m}^{-2}$) will be dependent on solution purity. However, any increase in J aimed at increasing QE will be accompanied by an

increase in cell voltage and perhaps energy consumption.

Fig. 5 shows the predicted variation of QE with T for both electrolytes with J and n held constant at 400 A m^{-2} and 40 s^{-1} , respectively. Surprisingly, both electrolytes exhibit a maximum at 45°C , although the curve is somewhat flatter for the very-high-purity electrolyte (~ 0.7 versus 1.0% range in QE for $20\text{--}70^\circ\text{C}$). Both Liebscher [4] and Ful'man and Khan [5] have reported similarly shaped curves with maxima at $\sim 38^\circ\text{C}$ for plant electrolytes ($J \simeq 600 \text{ A m}^{-2}$). Also, the latter authors [5] claimed that the optimum temperature for zinc electrowinning increased by $\sim 1^\circ\text{C}$ for an increase in J of $\sim 100 \text{ A m}^{-2}$, apparently based on statistical analysis of plant data. Salin *et al.* [3] showed that, while there is only a minor dependence of QE on T for high-purity electrolytes, an increase in T could be disastrous if the electrolyte contained high levels of certain impurities. Based on the present predictions, an increase in T from say 35 to 45°C for a high-purity electrolyte might be expected to result in a better QE and lower energy consumption, but these advantages may be offset by an increase in anode corrosion and an accompanying decrease in zinc purity in a conventional electrowinning cell.

4. Conclusions

The optimum conditions for zinc electrowinning in two synthetic zinc sulphate electrolytes have been identified using an approach based on the 'path of steepest ascent' of Box and Wilson [10, 11]. The utility of the method may be limited by the experimentally accessible region and the number of runs required. However, these problems can be overcome to an extent by the application of constrained optimization [14] and efficient experimental design [12]. The conditions under which the maxima in QE were obtained were very different for the two electrolytes studied, but the values of QE obtained were similar (98.8, 98.4%). The optimal conditions identified here for the very-high-purity electrolyte are far removed from, and would not be compatible with, present industrial practice. However, they do indicate that, under suitable circumstances, the electrodeposition of zinc

can be carried out efficiently at elevated temperatures, with the prospect of improved energy efficiency.

The statistical response surface model calculated during the optimization process allows the production of QE contours as a function of T , J and n . These contours are valuable in presenting an overview of electrolyte performance, giving more complete information than a series of 'one factor at a time' experiments. They also allow convenient comparison of the performance of different electrolytes over a wide range of conditions and may even be diagnostic for electrolytes containing particular types of impurities. For both electrolytes, the dominant factors determining QE were T and J . The interactions between n and J and T and J were statistically significant for the baseline and the very-high-purity electrolyte, respectively. There is little in the present work which can be compared with previous statistical studies [6–8] because of the different variables involved, but the reported significance of both J [6, 7] and T [8] is confirmed.

Once generated, the model of the surface can be used to predict the QE response under any set of conditions. While the reliability of the prediction can only be guaranteed for interpolation inside the experimental sub-region, limited extrapolation is mathematically possible and may provide indications of likely performance. In the present case, the QE responses for two electrolytes were examined under conditions closer to industrial practice ($T = 35^\circ\text{C}$, $J = 400 \text{ A m}^{-2}$); no data were available to estimate the effective n (i.e. mass transfer rate), but a value was chosen ($n = 40 \text{ s}^{-1}$) where the QE for the very-high-purity electrolyte was relatively insensitive to changes in n . While the overall performances of the two electrolytes were quite different with respect to J and T , the shape of the curve and the location of the optimum point for the QE versus T plot were the same for both. The characteristics of such curves (as with the contours) are a function of the electrolyte impurity composition. It was apparent that the QE response of the very-high-purity electrolyte was generally less dependent on J (in particular) and T than that observed for the electrolyte containing trace lead and nickel. Assuming that these trends would hold in the plant situation, where

mass transfer rates are presumably much lower, the present results suggest that greater flexibility would be possible in the setting of electrodeposition conditions as plant electrolyte purity is improved.

Acknowledgements

The authors wish to thank T. Biegler for discussions and advice, D. Albrecht for some computing assistance, and W. Kennedy and R. A. Pillig for technical assistance.

References

- [1] U. F. Turomshina and V. V. Stender, *J. Appl. Chem. USSR* **27** (1954) 1019.
- [2] G. N. Znamenskii and V. V. Stender, *ibid.* **33** (1960) 2692.
- [3] A. A. Salin, V. S. Volkova, Yu. N. Tokaev, I. P. Tulenkov, S. A. Kopytov and R. S. Guzairov, *Tsvet. Met.* **3** (12) (1962) 13.
- [4] R. Liebscher, *Neue Hutte* **14** (1969) 597.
- [5] N. I. Ful'man and O. A. Khan, *Tsvet. Met.* **18** (1) (1977) 20.
- [6] S. S. Kulikov, *Sov. Non-Ferrous Met. Res.* **9** (1981) 353.
- [7] R. C. Villas Bôas, 'Synergetic Phenomena in Zinc Electrowinning', National Science Foundation (USA) and Conselho Nacional De Desenvolvimento Cientifico E Tecnologico (Brazil), Rio de Janeiro (1977).
- [8] D. R. Fosnacht and T. J. O'Keefe, *Met. Trans. B* **14** (1983) 645.
- [9] T. Biegler and E. J. Frazer, *J. Appl. Electrochem.* **16** (1986) 654.
- [10] G. E. P. Box and K. B. Wilson, *J. Roy. Stat. Soc.* **13** (1951) 1.
- [11] O. L. Davies (ed.), 'The Design and Analysis of Industrial Experiments', 2nd edn, Oliver and Boyd, London (1967).
- [12] G. E. P. Box, W. G. Hunter and J. S. Hunter, 'Statistics for Experimenters', John Wiley & Sons, New York (1978).
- [13] T. Biegler and D. A. Swift, *Hydrometallurgy* **6** (1981) 299.
- [14] J. R. Nelder and R. Mead, *Computer J.* **7** (1965) 308.
- [15] P. G. Christie and W. J. Welch, in 'Extraction Metallurgy '81', Institution of Mining and Metallurgy (1981) p. 299.
- [16] A. W. Bryson, in 'Hydrometallurgy 81', Society of Chemical Industry, London (1981) p. G2/1.
- [17] A. Scott, R. M. Pitblado, O. M. G. Newman, J. Siemon and G. W. Barton, in 'Chemeca 85, Perth, August 1985', ICE, IEA and RACI, Australia (1985) p. 315.
- [18] R. C. Kerby and T. R. Ingraham, Mines Branch Research Report R243, Dept. of Energy, Mines and Resources, Ottawa, Canada (1971).
- [19] H. H. Fukubayashi, T. J. O'Keefe and W. C. Clinton, Bureau of Mines Report of Investigations 7966, US Dept. of the Interior (1974).
- [20] F. Ludwig, E. Yeager and G. Lozier, *Rev. Polarog. (Japan)* **14** (1967) 94.
- [21] G. C. Bratt, in 'The Aus. IMM Conference, Tasmania, May 1977', Australasian Institute of Mining and Metallurgy (1977) p. 277.
- [22] I. W. Wark, *J. Appl. Electrochem.* **9** (1979) 721.
- [23] A. A. Salin, *Tsvet. Met.* **2** (8) (1961) 29.